



Published in final edited form as:

Clin Exp Metastasis. 2008 ; 25(8): 893–901. doi:10.1007/s10585-008-9208-9.

Expressing connexin 43 in breast cancer cells reduces their metastasis to lungs

Zhongyong Li,

Division of Musculoskeletal Sciences, Department of Orthopaedics and Rehabilitation, The Pennsylvania State University College of Medicine, Hershey, PA 17033, USA

Zhiyi Zhou,

Division of Musculoskeletal Sciences, Department of Orthopaedics and Rehabilitation, The Pennsylvania State University College of Medicine, Hershey, PA 17033, USA

Danny R. Welch, and

Departments of Pathology, Cell Biology and Pharmacology/Toxicology, Comprehensive Cancer Center, University of Alabama at Birmingham, Birmingham, AL, USA

Henry J. Donahue

Division of Musculoskeletal Sciences, Department of Orthopaedics and Rehabilitation, The Pennsylvania State University College of Medicine, Hershey, PA 17033, USA

Abstract

Recently the concept that gap junctions play a role in cancer cell metastasis has emerged. However, the mechanism by which this might occur is unknown. To examine this issue a metastatic breast cancer cell line, MDA-MB-435, was stably transfected with human Cx43 cDNA. Four clones of 435 transfectants (435/Cx43⁺ c1, c6, c8, c14) and two clones of plasmid control (435/hy) were isolated and examined in this study. We found that expressing Cx43 in MDA-MB-435 cells decreased their expression of Cx32 but did not affect gap junctional intercellular communication, migration or invasion through Matrigel®. However, forced expression of Cx43 decreased the growth of MDA-MB-435 cells, decreased expression of N-cadherin, which is frequently associated with an aggressive phenotype, and increased MDA-MB-435 sensitivity to apoptosis. More importantly, there were fewer lung metastases in mice injected with 435/Cx43⁺ cells relative to mice injected with 435/hy. These results suggest that expressing Cx43 in breast cancer cells decreases their metastatic potential through a mechanism independent of gap junctional communication but, rather, related to N-cadherin expression and apoptosis.

Keywords

Apoptosis; Cadherins; Gap junctions; hTERT-HME1; MDA-MB-435

Introduction

Considerable evidence suggests that gap junctional intercellular communication (GJIC) and the expression of connexins, the protein sub units of gap junctional channels, are linked to tumorigenesis [1,2] and progression toward metastasis [3,4]. Several studies also suggest that GJIC and connexins contribute to suppression of tumor growth by participating in the

regulation of cell proliferation, differentiation and death [5-7]. Our previous data suggest that the highly metastatic breast cancer cell line MDA-MB-435 expresses connexin 32 (Cx32), but not connexin 43 (Cx43), while non tumorigenic non metastatic breast epithelial cells (hTERT-HME1) express Cx43 and connexin (Cx26), but no Cx32 [8]. We also found that MDA-MB-435 cells express phenotypic markers of osteoblastic cells including osteopontin, osteocalcin and Cbfa-1 [9]. Furthermore, we demonstrated that MDA-MB-435 cells expressing the metastasis suppressing gene BRMS1, display reduced expression of Cx32 and osteopontin and slightly restored Cx43 expression [8]. To further address the role of GJIC and connexin expression in tumorigenesis and metastasis, MDA-MB-435 cells were stably transfected with full length human Cx43 cDNA. Using these transfectants, we examined connexin expression, GJIC, cell number, apoptosis, invasion, migration and cadherin protein expression in vitro. In an in vivo study, we injected immunocompromised mice with MDA-MB-435 cells expressing Cx43 or controls and examined growth rates and size of orthotopic tumors as well as number of visible metastases in lungs recovered from injected mice.

Materials and methods

Reagents

All reagents were of analytical grade and commercially available. Monoclonal and polyclonal antibodies against Cx43, (catalog # 13-8300), N-cadherin (catalog # 33-3900), OB-cadherin (catalog # 32-1700) and E-cadherin (catalog # 13-1700) were purchased from Zymed (South San Francisco, USA). The oligonucleotides for the probes and primers for Cx43 were synthesized by Biosearch Technologies, Inc (Novata, USA). cDNA probes for Cx43, Cx26 and Cx32 were prepared as previously described [10,11]. The human osteoblastic cell line, hFOB 1.19, was provided by Steven Harris [12]. MDA-MB-435, hTERT-HME1 (human non cancer breast epithelial cells immortalized by infection with the retrovirus pBabepuro+hTERT vectorline) and HUV-EC-C (human umbilical vein endothelial cell line) were purchased from ATCC (Rockville, USA). pcDNA3.1/hygromycin B (-), hygromycin B, ampicillin, Top10 One Shot kits and Lipofectamine reagents were purchased from Invitrogen (Carlsbad, USA), BamHI, XbaI, KpnI and T4 DNA ligase from Boehringer Mannheim (Indianapolis, USA), and Qiaquick Gel Extraction, EndoFree Plasmid and RNeasy kits from Qiagen (Valencia, USA).

Development of Cx43 expressing MDA-MB-435 cells

A 1,817 bp fragment of human Cx43 cDNA [13] was ligated into the XbaI and KpnI sites of the pcDNA3.1/hygro (-) vector in the sense orientation. The sense orientation structure of pcDNA3.1/hygro (-)/human Cx43⁺ was analyzed and confirmed by sequence analysis (sequencer ABI model 377; Forster, CA) and was designated Cx43⁺. The plasmid vector control pcDNA3.1/hygro (-) was designated hy. For transfections, MDA-MB-435 cells were plated at 1×10^4 cells/mm² in 60 mm dishes containing 5 ml of Dulbecco's modified Eagle's medium (DMEM) with 10% fetal bovine serum (FBS) and incubated at 37°C, 5% CO₂ for 36 h. Cx43⁺ or hy (2 µg) were pre-complexed with 6 µl Plus reagent from the Lipofectamine reagent kit and incubated at room temperature for 15 min. Lipofectamine (12 µl) was added to DMEM (240 µl) before mixing with the pre-complex reagent containing either Cx43⁺ or hy, brought to a final volume of 260 µl with transfection medium and incubated at room temperature for 15 min. Prior to the addition of the transfection medium, MDA-MB-435 cells were washed once and maintained in 2 ml DMEM. Transfection medium (260 µl) was added to each MDA-MB-435 cell dish, mixed gently and incubated at 37°C, 5% CO₂. After a 3-h incubation, 2.26 ml of 20% FBS supplemented DMEM was added to the cells and the cells cultured 24 h. Following this 24-h incubation, the medium was replaced with selection medium containing 300 µg/ml hygromycin B and cultured for

10 to 14 days with medium replacement at 3-day intervals until resistant colonies were clearly visible. Resistant colonies (approximately 100-200 cells) were released from the culture, using trypsin, within plastic colonizing cylinders. The cells were sub-cultured in maintenance medium containing 150 µg/ml hygromycin B until sufficient numbers of cells (approximately 1×10^7) were obtained. Routine growth conditions included incubation at 37°C, 5% CO₂ and medium replacement with maintenance medium at 3-day intervals. Twenty six clones of MDA-MB-435 cells transfected with Cx43⁺ (435/Cx43⁺) and six clones of MDA-MB-435 cells transfected with hy (435/hy) were obtained. All clones were characterized and screened by real time reverse transcriptase polymerase chain reaction (RT-PCR) with Cx43 primers and probe, western blot with Cx43 antibody and cell coupling by fluorescence activated cell sorting (FACS). Four clones of 435/Cx43⁺ (c1, c6, c8 and c14) expressing higher levels of Cx43 mRNA, Cx43 protein and GJIC and two clones of plasmid control 435/hy5 (hy5) and 435/hy6 (hy6) were selected for this study. One more control, hy4, was added for in vivo metastasis assay.

Quantification of gap functional intercellular communication (GJIC)

GJIC was assessed by dual label dye transfer and fluorescent activated cell sorting (FACS) as previously described [8,14,15]. Briefly, donor cells were double-labeled by a 30-min exposure to the gap junction permeable dye calcein AM (10 µM/ml) and the lipophilic dye DiI (8.75 µg/mlM) (Molecular Probes, Eugene, OR) in HBSS containing 1% BSA and Pluronic F-127 (Molecule Probes). After one washing with PBS, donor cells were released with trypsin and 1×10^4 of these double labeled donor cells were dropped on top of a layer of unlabeled acceptor cells and the co-culture incubated for 2 h at 37°C and 5% CO₂. The co-cultures were then released with trypsin. After fixation with 2% paraformaldehyde for 15 min cells were resuspended in FACS buffer and assessed by FACS analysis.

Invasion and migration assay

A BioCoat FluoroBlok Invasion System (with Matrigel® coated multiwell inserts) and FluoroBlok Multiwell insert system (with uncoated multiwell inserts, both from Becton Dickinson Labware, Bedard, USA) were used to examine cell invasion and migration, respectively. Briefly, Matrigel® coated multiwell inserts for invasion assays were rehydrated with 0.5 ml of PBS at 37°C followed by incubation at 37°C in an incubator, without CO₂, for 2 h. Multiwell inserts for migration assays were not rehydrated. For both invasion and migration assays hTERT-HME1 cells and clones of 435/Cx43⁺ and 435/hy were cultured until confluent. On the day of the experiment cells were released with trypsin and suspended in culture medium without serum. A suspension of cells at 2.5×10^4 cells per 0.5 ml media was added to the top of the invasion or migration inserts and 0.75 ml of culture medium containing 10% FBS was added to the bottom chamber, as a chemo attractant, and the chamber incubated for 22 h. The medium was removed from the upper chamber, and the invading cells or migrating cells on the bottom of the insert well were stained with 1 mM calcein for 1 h in an incubator (37°C, 5% CO₂). The extra calcein dye was removed by immersing the insert wells into a fresh 24-well plate containing PBS. Invasion or migration of cells was assessed by reading the fluorescence of invading or migrating cells using a fluorescence plate reader at excitation/emission wave-lengths of 485/530 nm.

Quantitative analysis of protein levels by Western blot

Steady state level of protein was assessed by Western blot analysis. Total cellular protein was assessed using antibodies against Cx43, E-cadherin, N-cadherin, OB-cadherin and, as a control, glyceraldehyde-3-phosphate dehydrogenase (GAPDH; purchased from Accurate Chemical and Scientific Corp. Westbury USA; catalog # YBG6999555) as previously described [13]. Equivalent amounts of each protein (40 µg) were applied to 10% pre-cast SDS-polyacrylamide gels (Bio-Rad, Hercules, USA) at 100 volts for 1.5 h and transferred to

nitrocellulose membranes at 40 volts overnight at 4°C. The membranes were blocked by a blocking solution containing 5% non-fat milk, 0.05% Tween-20 Tris-Buffered-Saline (TBS; (Bio-Rad) for 1 h before incubation for 3 h at room temperature with each antibody (diluted 1:1,000 to 1:500 in blocking solution). The membranes were washed three times with 0.05% Tween-20 TBS and incubated for 1 h with goat anti-mouse (for monoclonal antibodies) or goat anti-rabbit (for polyclonal antibodies) IgG linked to horseradish peroxidase (Bio-Rad) diluted 1:3,000 in blocking solution. After three additional washes with 0.05% Tween-20 TBS, membranes were soaked in enhanced chemiluminescence (ECL) detection reagents (Amersham, UK). The membranes were then air-dried and exposed to X-ray film. Densitometry measurements were performed using a Bio-Rad Q-one program (Bio-Rad). Data from optical density readings of protein were normalized to GAPDH.

Quantitative real-time RT-PCR

Total RNA was isolated from each cell line using a Qiagen RNeasy mini kit. Gene Expression was quantified by realtime RT-PCR using an Applied Biosystems 7300 Real-Time PCR System (Applied Biosystems, Foster City, USA) as previously described [13]. Primers and probes were designed using sequence data from Genbank and the real-time PCR probe/primer design software Primer Express (version 1.0, Applied Biosystems). The sequences of primers and probes are as follow: for Cx43; forward primer 5'GCT CCT CAC CAA CCG CT3', reverse primer 5'TTG CGG CAG GAG GAA TTG3' and probe TCT CAC CTA TGT CTC CTC CTG GGT ACA A3' (NM_000166). For Cx32; forward primer CAA CAG CGT TTG CTA TGA CCA C3', reverse primer 5'-TGA GCT GCA GGG ACC ACA and probe CTT CCC CAT CTC CCA TGT GCG G (NM_000166). For real time qPCR analysis, DNase-treated RNA was reverse-transcribed using High Capacity cDNA Reverse Transcription kit (Applied Biosystems, Foster City, CA) and the protocol provided with the kit. Quantification by real-time PCR was accomplished by adding 10 or 20 ng of cDNA in a reaction with 2× TaqMan Universal PCR Master Mix (Applied Biosystems, Foster City, USA) in a volume of 20 µl. Primer was added at a concentration of 400 nM and a probe which was labeled with a 5' FAM and a 3' Black Hole Quencher (Biosearch Tech, Novato, CA) was added at 200 nM. The amplification protocol consisted of 2 min at 50°C and 10 min at 95°C, followed by 40 cycles of 15 s at 95°C and 1 min at 60°C. Ct values of genes of interest and the reference gene 18S were calculated using the delta Ct method to determine relative steady state mRNA levels.

Cell number and caspase-3-activity

0.5×10^5 cells were seeded into 10 mm dishes and cultured for 3 days. Cell numbers were quantified at 3 days using a hemocytometer. Caspase-3 activity was quantified using a Caspase-3 Fluorescent Assay kit (Clontech Laboratories, Inc, Palo Alto, USA) according to the manufactures instructions. Briefly, cells were cultured in 0.2% FCS culture medium with 1 µM retinoic acid (RA) for 9 days before the assay. On the day of assay, 1×10^6 cells were suspended in chilled cell lyses buffer supplied in the kit and incubated for 10 min on ice. Cell lysates were centrifuged in a micro centrifuge at maximum speed for 3 min at 4°C to precipitate cell debris and the supernatants transferred to a new tube. 50 µl of 2× Reaction buffer/DTT mix and 1 µl of DEVD-Cho inhibitor were added to 50 µl of the supernatant which was then mixed and incubated at 37°C for 30 min in a shaking water bath. Other samples were kept on ice. After 30 min of shaking, 50 µl of 2× Reaction buffer/DTT mix was added to each reaction. Then, 5 µl of 1 mM caspase-substrate was added to each sample, including control, and the samples were placed in a 37°C water bath for 1 h. A calibration curve was generated using standards provided by the manufacture. Finally, all samples were transferred to a 96-well plate and read by a fluorometer (Bio-Rad, Hercules, USA) with 400 nm excitation and 505 nm emission filters.

In vivo tumorigenesis and metastasis

Spontaneous metastases was quantified as previously described [16]. Briefly, 56 athymic nu/nu-Foxn1(nu) mice (Harlan, Indianapolis, USA) were randomly placed into two groups: 32 mice for 435/Cx43⁺ (c1, c6, c8 and c14) and 24 mice for plasmid control 435/hy (hy4, hy5, hy6) and cells from each clonal line were injected into eight mice. 1×10^6 cells of each clone were injected into exposed axillary mammary fat pads of anesthetized 5- to 6-week-old female mice. To estimate tumorigenicity, orthotopic tumor size (OTS) was quantified starting 1 week after injection. The growth rate was monitored by diameter measurement of orthotopic tumor. When the mean tumor diameter reached 1.2-1.5 cm, tumors were surgically removed under ketamin:xylazine (80-85 mg/kg:14-16 mg/kg) anesthesia and the wounds were closed with sterile stainless steel clips. Two months later, mice were killed and examined for the presence of metastases. Lungs were removed, rinsed in water, and fixed in Bouin's solution before quantification of surface metastases as described previously [16,17]. We did not section lungs or examine lungs histologically as we have verified previously that metastases on lung surfaces account for greater than 80% of metastases due to the lungs anatomy [17].

Statistical analysis

All experiments were performed in duplicate, and in some cases triplicate, at least four times. Data are from four clones of Cx43 transfectants, two clones of plasmid control, except in the case of in vivo experiments where three clones of plasmid controls were injected, and hTERT-HME1 cells. All data are reported as the mean \pm SEM. Statistical significance was assessed by one-way analysis of variance (ANOVA) followed by a student-Newman-Keuls test and $P < 0.05$ was considered significant.

Results

Quantitative analysis of steady state protein and mRNA levels by Western blot and real time RT-PCR, respectively, revealed that Cx43 protein and Cx43 mRNA were expressed in all clones of 435/Cx43⁺ including c1, c6, c8 and c14 as well as in human breast epithelial cells hTERT-HME1. However, Cx43 was not detected in 435/hy and (Fig. 1a). Cx43 protein and mRNA in 435/Cx43⁺ were significantly increased relative to 435/hy (Fig. 1b, c). Cx43 mRNA in hTERT-HME1 was greater than in 435/hy cells but lower than in 435/Cx43⁺ (Fig. 1c). Steady state Cx32 mRNA levels were significantly decreased in 435/Cx43⁺ relative to 435/hy cells while Cx32 was not detected in hTERT-HME1 (Fig. 1d). GJIC in hTERT-HME1 was greater than in any of the other cell lines examined while it was similar in 435/Cx43⁺ and 435/hy (Fig. 1e).

Invasion and migration were similar in all cell lines examined (Fig. 2a, b). However, the number of 435/Cx43⁺, as assessed by cell counts, was significantly decreased relative to that in 435/hy. The number of hTERT-HME1 and 435/Cx43⁺ was similar (Fig. 2c). Caspase-3 activity in 435/Cx43⁺ was significantly increased relative to that in 435/hy (Fig. 2d).

Western blot analysis revealed that all clones of 435/Cx43⁺, 435/hy and hTERT-HME1 cells expressed OB-cadherin (Fig. 3a) and N-cadherin (Fig. 3b) proteins albeit at different abundances. Levels of OB-cadherin protein in 435/Cx43⁺ and 435/hy were not statistically different from one another, but both were significantly decreased relative to hTERT-HME1 cells (Fig. 3c). Levels of N-cadherin protein in 435/Cx43⁺ were significantly decreased relative to those in 435/hy. hTERT-HME1 cells expressed a very small amount of N-cadherin protein (Fig. 3d). E-cadherin protein was detected only in hTERT-HME1 (data not shown).

In vivo data revealed that OTS on day 7 post-injection was similar in mice injected with either 435/Cx43⁺ or 435/hy. However, at 30 days post injection mice injected with 435/Cx43⁺ cells had slightly, but statistically significant, larger tumors than mice injected with 435/hy while 60 days post-injection, mice injected with 435/Cx43⁺ had slightly, but statistically significant, smaller tumors than mice injected with 435/hy (Fig. 4a). More importantly, the number of metastases recovered in lungs of nude mice injected with 435/Cx43⁺ was significantly decreased (nearly 50%) relative to mice injected with 435/hy (Fig. 4b).

Discussion

In support of previous studies reported in the literature [18], including our own [8], we found that Cx43 levels were reduced in breast cancer cells relative to non cancerous breast epithelial cells. On the other hand, Cx32 levels were up regulated in breast cancer cell lines, relative to non cancerous breast epithelial cells, and expressing Cx43 in breast cancer cell lines resulted in a decrease in Cx32 expression. These findings suggest that the connexin expression profile changes as breast epithelial cells transition to cancerous cells and that there is an inverse relationship between Cx43 and Cx32 expression in breast epithelial cells and breast cancer cells.

Recent studies from our laboratory suggest that expressing Cx43 in breast cancer cells decreases their invasion through Matrigel® and adhesion to endothelial cells [15] suggesting that expressing Cx43 would alter the metastatic potential of breast cancer cells. To address this we injected our Cx43 expressing breast cancer cells into immunocompromised mice. Sixty days after injection the tumor size in mice injected with Cx43 expressing cells was significantly reduced relative to tumor size in mice injected with vector controls. These results are consistent with those reported by Hirsch et al. [19] showing that expressing Cx43 in MDA-MB-435 cells results in growth suppression and similar, although less dramatic, to results reported by Qin et al. [20] demonstrating that over expression of Cx43 in another breast cancer cell line, MDA-MB-231, results in decreased tumor growth in mice. Additionally, we also found that the number of metastases to lungs was reduced in mice injected with Cx43 expressing breast cancer cells relative to mice injected with vector controls. It is possible that the decreased metastasis observed in mice injected with 435/Cx43⁺ cells, relative to mice injected with 435/hy cells, was at least partly due to the decreased size of the tumor in these mice at 60 days. However, it is unlikely that the decreased tumor size in mice injected with 435/Cx43⁺ was, by itself, responsible for the decreased metastasis. While mice injected with 435/Cx43⁺ had tumors 13% smaller than in those injected with 435/hy, the number of metastases was reduced nearly 55%. This suggests that at least some of the decreased metastasis in mice injected with 435/Cx43⁺ was independent of the decreased tumor size in these mice. Taken together these results support the concept that decreased Cx43 expression contributes to tumorigenesis and offer the first direct in vivo evidence that decreased Cx43 plays a role in metastasis.

To examine the mechanism by which decreased Cx43 expression contributes to breast cancer cell metastasis we first examined homotypic GJIC within each cell line examined. Interestingly, GJIC was reduced in 435/hy breast cancer cells, but increasing Cx43 expression in these cells did not restore GJIC. This is consistent with previous findings from our laboratory as well as others [15,20]. While Cx43 levels in stably transfected 435/Cx43⁺ clones were lower than in hTERT, they were increased relative to levels in 435/hy. The decreased expression in 435/hy cells, a breast cancer cell line, relative to hTERT, a model for “normal” breast epithelial, is consistent with previous reports of decreased Cx43 levels in breast cancer cells as they become tumorigenic [21]. Expressing Cx43 in 435 cells increases their Cx43 expression and but did not restore GJIC. This suggests that in addition

to a decreased expression of Cx43 protein in 435/hy cells relative to hTERT cells there is a post translational defect (e.g. impaired trafficking of connexins to the membrane and formation of connexons, impaired docking with adjacent connexons, or impaired channel gating) in 435/hy cells, that is not alleviated by expressing Cx43 in 435/Cx43⁺ cells, that precludes full restoration of GJIC. In any case, these results suggest that the anti tumorigenic and anti metastatic effect of Cx43 expression is independent of GJIC.

We previously demonstrated that restoring Cx43 expression in another breast cancer cell line, MDA-MB-231, decreased invasion through Matrigel® and adhesion to human umbilical vein endothelial cells but did not affect migration. In this study, we found a similar trend towards a decrease in Matrigel® invasion in Cx43 expressing MDA-MB-435 cells but this did not reach statistical significance nor did the change in cell migration. Therefore, it is unlikely that changes in processes involved in Matrigel® invasion contribute to the decreased metastasis in Cx43 expressing MDA-MB-435 cells.

We next examined cadherin expression in breast cancer cell lines. Several studies have demonstrated that E-cadherin expression is decreased in invasive breast carcinomas and is directly related to connexin expression [22-24]. We detected E-cadherin in non cancerous breast epithelial cells but did not detect it in breast cancer cell lines even when Cx43 was over expressed. We recently demonstrated that Cx43 expression in MDA-MB-231 results in decreased expression of OB-cadherin [15] and found a similar trend in Cx43 expressing MDA-MB-435 cells but this did not reach statistical significance. However, we did detect a significant decrease in N-cadherin in Cx43 expressing MDA-MB-231 cells. N-cadherin is involved in increased motility, invasion and metastases of breast cancer cells [25,26] and thus the decreased expression of N-cadherin in Cx43 over expressing MDA-MB-435 cells may contribute to decreased metastasis in vivo.

Emerging evidence suggests that Cx43 plays a role in apoptosis, but what that role is may be different in different cell systems. For instance, Huang et al. demonstrated that Cx43 enhances apoptosis in response to chemotherapeutic agents [27] or low serum conditions [28] in human glioblastoma cells. On the other hand Cx43 is necessary for the anti apoptotic effect of bisphosphonates [29] and camptothecin induced apoptosis is greater in Cx43 deficient osteoblastic cells [30]. There are no direct studies of the role of Cx43 in breast cancer cell apoptosis. However, it has been demonstrated that Cx43 expression is directly correlated with the expression of BAK (Bcl-2 homologous antagonist/killer), a pro-apoptotic gene of the Bcl-2 family, in human breast cancer tissue [31]. To more directly address this issue we examined retinoic acid induced caspase activity in breast cancer cells expressing Cx43. We found that breast cancer cells expressing Cx43 were more sensitive to the apoptosis inducing effect of retinoic acid than breast cancer cells with less expression of Cx43. These results should be interpreted with caution as retinoic acid also increases GJIC in several cell lines including human mammary-carcinoma MCF-7[32] However, Saez et al. [32] also reported that the effect of retinoic acid on GJIC was unrelated to its effect on apoptosis. Interestingly, an inverse relationship between N-cadherin expression and apoptosis has also been reported in several cancer cell lines [33,34] Thus the anti metastatic effect of Cx43 may be related to decreased expression of N-cadherin and enhanced sensitivity to apoptosis.

It is important to note that the origin of MDA-MB-435 cells has recently been called into question with some data suggesting that MDA-MB-435 cells are actually melanocytes [35,36]. However, MDA-MB-435 cells have been demonstrated to express milk proteins and metastasize from mammary fat pad but not subcutaneous tissue consistent with the cell line being a breast carcinoma [17,37]. Even if MDA-MB-435 cells are not authentic breast

cancer cells it would not alter our interpretation of the data suggesting that Cx43 contributes to cancer cell metastasis.

In summary, our data suggest that expressing Cx43 in breast cancer cells, which normally express very little if any Cx43, decreased their metastatic potential to lung. Interestingly, this appeared to be independent of changes in invasion, migration or GJIC. Rather, it is more likely related to a decrease in N-cadherin expression resulting in an increased sensitivity to apoptosis.

Acknowledgments

This work was supported by the National Institute of Health grants CA90991 and AG13087 to Henry J. Donahue and CA87228 to Danny R. Welch.

Abbreviations

GJIC	Gap junctional intercellular communication
Cx	Connexin

References

- Loewenstein WR, Kanno Y. Intercellular communication and the control of tissue growth: lack of communication between cancer cells. *Nature* 1966;209(29):1248–1249. [PubMed: 5956321]
- Yamasaki H, Mesnil M, Omori Y, et al. Intercellular communication and carcinogenesis. *Mutat Res—Fundam Mol Mech Mutagen* 1995;333(1-2):181–188.
- Ito A, Katoh F, Kataoka TR, et al. A role for heterologous gap junctions between melanoma and endothelial cells in metastasis. *J Clin Invest* 2000;105(9):1189–1197. [PubMed: 10791993]
- Nicolson GL, Dulski KM, Trosko JE. Loss of intercellular junctional communication correlates with metastatic potential in mammary adenocarcinoma cells. *Proc Natl Acad Sci USA* 1988;85(2):473–476. [PubMed: 3422438]
- Zhang J, Li W, Sumpio BE, et al. Fibronectin blocks p38 and jnk activation by cyclic strain in Caco-2 cells. *Biochem Biophys Res Commun* 2003;306(3):746–749. [PubMed: 12810082]
- Krutovskikh VA, Troyanovsky SM, Piccoli C, et al. Differential effect of subcellular localization of communication impairing gap junction protein connexin43 on tumor cell growth in vivo. *Oncogene* 2000;19(4):505–513. [PubMed: 10698520]
- Mehta P, Perez-Stable C, Nadji M, et al. Suppression of human prostate cancer cell growth by forced expression of connexin genes. *Dev Genet* 1999;24(1-2):91–110. [PubMed: 10079514]
- Saunders MM, Seraj MJ, Li Z, et al. Breast cancer metastatic potential correlates with a breakdown in homospecific and heterospecific gap junctional intercellular communication. *Cancer Res* 2001;61(5):1765–1767. [PubMed: 11280719]
- Kapoor P, Suva LJ, Welch DR, et al. Osteoprotegerin and the bone homing and colonization potential of breast cancer cells. *J Cell Biochem* 2008;103(1):30–41. [PubMed: 17471510]
- Li Z, Zhou Z, Daniel EE. Expression of gap junction connexin 43 and connexin 43 mRNA in different regional tissues of intestine in dog. *Am J Physiol* 1993;265:G911–G916. [PubMed: 8238521]
- Li Z, Zhou Z, Yellowley CE, et al. Inhibiting gap junctional intercellular communication alters expression of differentiation markers in osteoblastic cells. *Bone* 1999;25(6):661–666. [PubMed: 10593410]
- Harris SA, Enger RJ, Riggs BL, et al. Development and characterization of a conditionally immortalized human fetal osteoblastic cell line. *J Bone Miner Res* 1995;10(2):178–186. [PubMed: 7754797]

13. Li Z, Zhou Z, Saunders MM, et al. Modulation of connexin43 alters expression of osteoblastic differentiation markers. *Am J Physiol Cell Physiol* 2006;290(4):C1248–C1255. [PubMed: 16319124]
14. Kapoor P, Saunders MM, Li Z, et al. Breast cancer metastatic potential: correlation with increased heterotypic gap junctional intercellular communication between breast cancer cells and osteoblastic cells. *Int J Cancer* 2004;111(5):693–697. [PubMed: 15252837]
15. Li Z, Zhou Z, Donahue HJ. Alterations in Cx43 and OB-cadherin affect breast cancer cell metastatic potential. *Clin Exp Metastasis* 2008;25(3):265–272. [PubMed: 18193170]
16. Seraj MJ, Samant RS, Verderame MF, et al. Functional evidence for a novel human breast carcinoma metastasis suppressor, BRMS1, encoded at chromosome 11q13. *Cancer Res Adv Brief* 2000;60:2764–2769.
17. Welch DR. Technical considerations for studying cancer metastasis in vivo. *Clin Exp Metastasis* 1997;15(3):272–306. [PubMed: 9174129]
18. McLachlan E, Shao Q, Laird DW. Connexins and gap junctions in mammary gland development and breast cancer progression. *J Membr Biol* 2007;218(1-3):107–121. [PubMed: 17661126]
19. Hirschi KK, Xu CE, Tsukamoto T, et al. Gap junction genes Cx26 and Cx43 individually suppress the cancer phenotype of human mammary carcinoma cells and restore differentiation potential. *Cell Growth Differ* 1996;7(7):861–870. [PubMed: 8809403]
20. Qin H, Shao Q, Curtis H, et al. Retroviral delivery of connexin genes to human breast tumor cells inhibits in vivo tumor growth by a mechanism that is independent of significant gap junctional intercellular communication. *J Biol Chem* 2002;277(32):29132–29138. [PubMed: 12042301]
21. Laird DW, Fistouris P, Batist G, et al. Deficiency of connexin43 gap junctions is an independent marker for breast tumors. *Cancer Res* 1999;59(16):4104–4110. [PubMed: 10463615]
22. Jongen WMF, Fitzgerald DJ, Asamoto M, et al. Regulation of connexin 43-mediated gap junctional intercellular communication by Ca^{2+} in mouse epidermal cells is controlled by E-cadherin. *J Cell Biol* 1991;114(3):545–555. [PubMed: 1650371]
23. Prowse DM, Cadwallader GP, Pitts JD. E-cadherin expression can alter the specificity of gap junction formation. *Cell Biol Int* 1997;21(12):833–843. [PubMed: 9812347]
24. Terzaghi-Howe M, Chang GW, Popp D. Emergence of undifferentiated rat tracheal cell carcinomas, but not squamous cell carcinomas, is associated with a loss of expression of E-cadherin and of gap junction communication. *Carcinogenesis* 1997;18(11):2043–2050. [PubMed: 9395200]
25. Nieman MT, Prudoff RS, Johnson KR, et al. N-cadherin promotes motility in human breast cancer cells regardless of their E-cadherin expression. *J Cell Biol* 1999;147(3):631–644. [PubMed: 10545506]
26. Hazan RB, Phillips GR, Qiao RF, et al. Exogenous expression of N-cadherin in breast cancer cells induces cell migration, invasion, and metastasis. *J Cell Biol* 2000;148(4):779–790. [PubMed: 10684258]
27. Huang RP, Hossain MZ, Huang R, et al. Connexin 43 (cx43) enhances chemotherapy-induced apoptosis in human glioblastoma cells. *Int J Cancer* 2001;92(1):130–138. [PubMed: 11279616]
28. Huang R, Liu YG, Lin Y, et al. Enhanced apoptosis under low serum conditions in human glioblastoma cells by connexin 43 (Cx43). *Mol Carcinog* 2001;32(3):128–138. [PubMed: 11746825]
29. Plotkin LI, Bellido T. Bisphosphonate-induced, hemi-channel-mediated, anti-apoptosis through the Src/ERK pathway: a gap junction-independent action of connexin43. *Cell Commun Adhes* 2001;8(4-6):377–382. [PubMed: 12064622]
30. Castro CH, Stains JP, Sheikh S, et al. Development of mice with osteoblast-specific connexin43 gene deletion. *Cell Commun Adhes* 2003;10(4-6):445–450. [PubMed: 14681055]
31. Kanczuga-Koda L, Sulkowski S, Tomaszewski J, et al. Connexins 26 and 43 correlate with Bak, but not with Bcl-2 protein in breast cancer. *Oncol Rep* 2005;14(2):325–329. [PubMed: 16012710]
32. Saez CG, Velasquez L, Montoya M, et al. Increased gap junctional intercellular communication is directly related to the anti-tumor effect of all-trans-retinoic acid plus tamoxifen in a human mammary cancer cell line. *J Cell Biochem* 2003;89(3):450–461. [PubMed: 12761879]

33. Gwak GY, Yoon JH, Yu SJ, et al. Anti-apoptotic N-cadherin signaling and its prognostic implication in human hepatocellular carcinomas. *Oncol Rep* 2006;15(5):1117–1123. [PubMed: 16596172]
34. Tran NL, Adams DG, Vaillancourt RR, et al. Signal transduction from N-cadherin increases Bcl-2. Regulation of the phosphatidylinositol 3-kinase/Akt pathway by homophilic adhesion and actin cytoskeletal organization. *J Biol Chem* 2002;277(36):32905–32914. [PubMed: 12095980]
35. Rae JM, Creighton CJ, Meck JM, et al. MDA-MB-435 cells are derived from M14 melanoma cells—a loss for breast cancer, but a boon for melanoma research. *Breast Cancer Res Treat* 2007;104(1):13–19. [PubMed: 17004106]
36. Lacroix M. Persistent use of “false” cell lines. *Int J Cancer* 2008;122(1):1–4. [PubMed: 17960586]
37. Sellappan S, Grijalva R, Zhou X, et al. Lineage infidelity of MDA-MB-435 cells: expression of melanocyte proteins in a breast cancer cell line. *Cancer Res* 2004;64(10):3479–3485. [PubMed: 15150101]

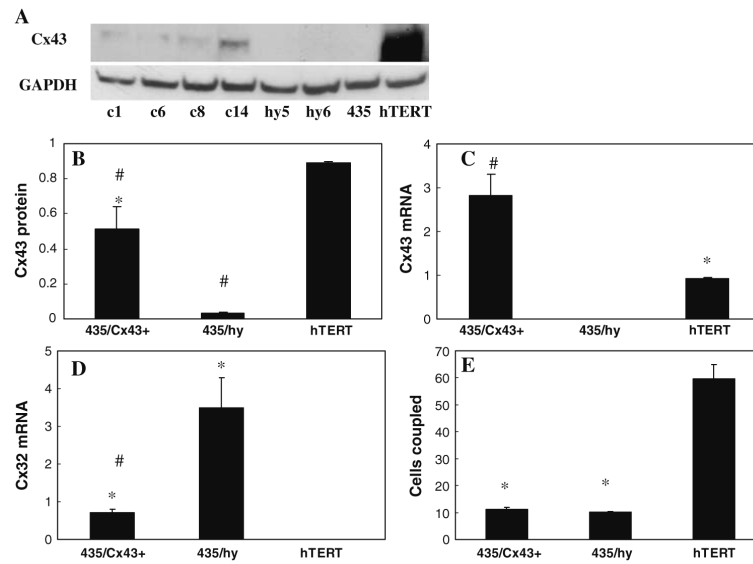


Fig. 1. Connexin expression and gap junctional intercellular communication. **(a)** Protein isolated from cells was analyzed by Western blot with a Cx43 polyclonal antibody and re-blotted for glyceraldehyde-3-phosphate dehydrogenase (GAPDH). A 43-kd band of Cx43 protein was detected in c1, c6, c8, c14 and hTERT-HME1 cells, but not in 435, hy5 and hy6 cells. Photograph represents a typical result from five similar gels. **(b)** Densitometric analysis of Western blots to detect Cx43 protein levels. Values represent the average of the ratio of Cx43 protein to GAPDH protein from each cell line. Four clones of 435/Cx43⁺ (c1, c6, c8, c14), two clones of the 435/hy plasmid control (hy5 and hy6) and hTERT-HME1 cells were examined. *Significantly greater than 435/hy, #significantly less than hTERT. **(c)** and **(d)** Real time reverse transcriptase-polymerase chain reaction (RT-PCR) analysis of steady state mRNA levels of Cx43 and Cx32. Total RNAs isolated from cells of four clones of 435/Cx43⁺ (c1, c6, c8 and c14), two clones of the plasmid control 435/hy (hy5 and hy6) and hTERT-HME1, were applied to RT-PCR with probes and primers of Cx43 and Cx32. Values represented mRNA levels relative to 18S controls. **(c)** #Significantly greater than 435/hy and hTERT-HME1, *significantly greater than 435/hy. **(d)** *Significantly greater than hTERT, #significantly less than 435/hy. **(e)** Homotypic gap junctional intercellular communication. Cells were cultured and subjected to a dual-label dye transfer assay and assessed by FACS as described in materials and methods. *Significantly less than hTERT-HME1. Values are mean \pm SEM, $P < 0.05$, $n = 6-12$

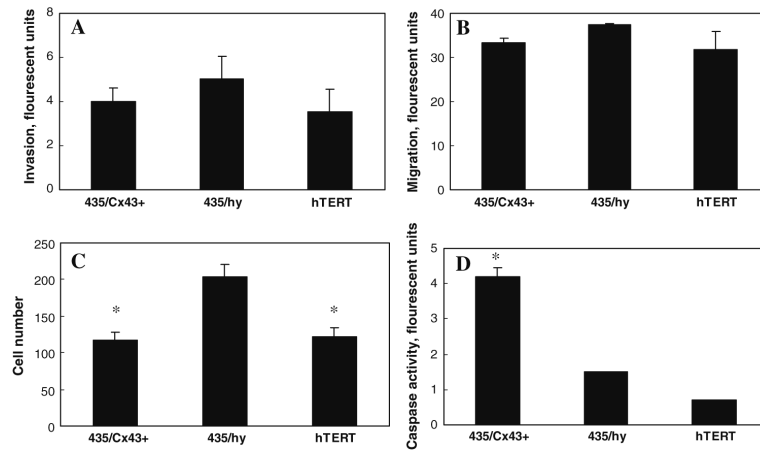
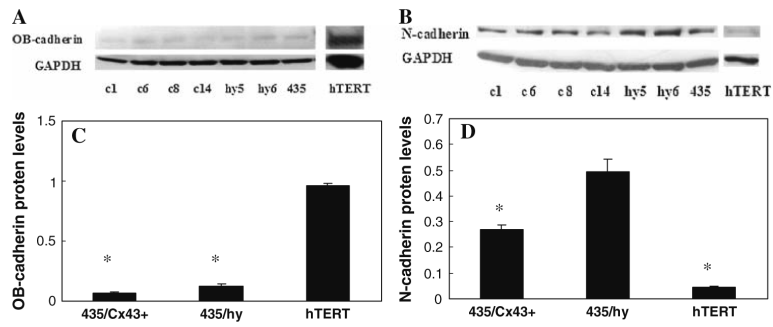


Fig. 2. Cellular invasion, migration, number and apoptosis. (a) and (b) Fluorescent units reflecting number of invading, through Matrigel®, or migrating cells. Invasion and migration were similar in all cells examined, $n = 18$. (c) Cell number as determined by cell counts. *Significantly less than 435/hy, $n = 4$. (d) Apoptosis as assessed by caspase-3 activity, fluorescent units reflect caspase activity. *Significantly greater than either 435/hy or hTERT-HME1, $n = 3$

**Fig. 3.**

OB-cadherin and N-cadherin protein levels. Protein isolated from four clones of 435/Cx43⁺ (c1, c6, c8, c14), two clones of the 435/hy plasmid control (hy5 and hy6), 435 and hTERT-HME1 cells was analyzed by Western blot with antibodies against OB-cadherin (a) and N-cadherin (b) and re-blotted for glyceraldehyde-3-phosphate dehydrogenase (GAPDH). OB-cadherin protein and N-cadherin protein bands were found in all cell lines examined. Photograph represents a typical result from five similar gels. (c) and (d) Values represent the average of the ratio of OB-cadherin or N-cadherin protein density to GAPDH protein density. (c) *Significantly less than hTERT-HME1, $n = 4$. (d) *Significantly less than 435/hy, $n = 3$

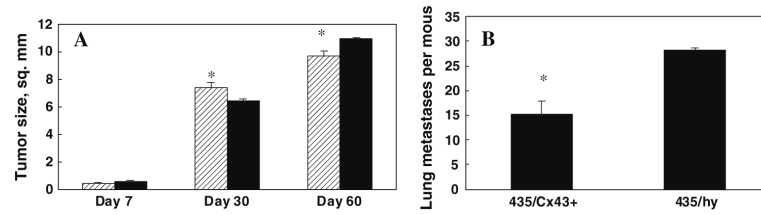


Fig. 4.

In vivo tumorigenicity and metastasis. **(a)** Orthotopic tumor size in mice injected with clones of 435/Cx43⁺ or 435/hy. *Significantly different than 435/hy on the same day. **(b)** The number of visible metastases in lungs from mice injected with 435/Cx43⁺ was significantly less than in lungs from mice injected with 435/hy. *Significantly less than 435/hy injected mice, $n = 24-32$